Title

Reorientation of the Methyl Group in MAs(III) is the Rate-Limiting Step in the ArsM As(III) S-Adenosylmethionine Methyltransferase Reaction



Journal

ACS Omega, 3(3)

ISSN

2470-1343

Authors

Packianathan, Charles

Li, Jiaojiao

Kandavelu, Palani

et al.

Publication Date

2018-03-31

DOI

10.1021/acsomega.8b00197

Peer reviewed

ACS OMEGA

Article

Cite This: ACS Omega 2018, 3, 3104−3112

# Reorientation of the Methyl Group in MAs(III) is the Rate-Limiting Step in the ArsM As(III) *S*-Adenosylmethionine Methyltransferase Reaction

Charles Packianathan,[†] Jiaojiao Li,[†] Palani Kandavelu,[‡] Banumathi Sankaran,[§] and Barry P. Rosen*[,†]

[†]Department of Cellular Biology and Pharmacology, Herbert Wertheim College of Medicine, Florida International University, Miami, Florida 33134, United States

[‡]SER-CAT and the Department of Biochemistry and Molecular Biology, University of Georgia, Athens, Georgia 30602, United States

[§]Molecular Biophysics and Integrated Biology, Lawrence Berkeley Laboratory, Berkeley, California 94720, United States

Supporting Information

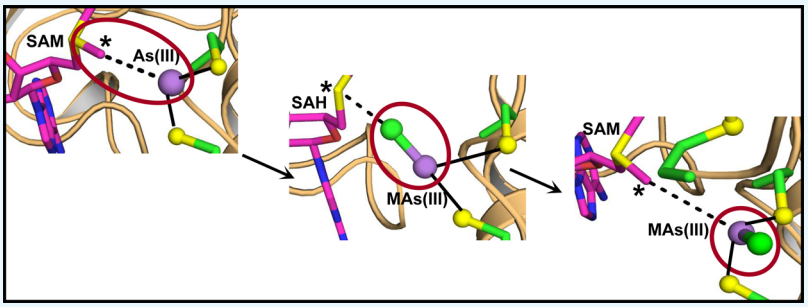


**ABSTRACT:** The most common biotransformation of trivalent inorganic arsenic (As(III)) is methylation to mono-, di-, and trimethylated species. Methylation is catalyzed by As(III) *S*-adenosylmethionine (SAM) methyltransferase (termed ArsM in microbes and AS3MT in animals). Methylarsenite (MAs(III)) is both the product of the first methylation step and the substrate of the second methylation step. When the rate of the overall methylation reaction was determined with As(III) as the substrate, the first methylation step was rapid, whereas the second methylation step was slow. In contrast, when MAs(III) was used as the substrate, the rate of methylation was as fast as the first methylation step when As(III) was used as the substrate. These results indicate that there is a slow conformational change between the first and second methylation steps. The structure of CmArsM from the thermophilic alga *Cyanidioschyzon merolae* sp. 5508 was determined with bound MAs(III) at 2.27 Å resolution. The methyl group is facing the solvent, as would be expected when MAs(III) is bound as the substrate rather than facing the SAM-binding site, as would be expected for MAs(III) as a product. We propose that the rate-limiting step in arsenic methylation is slow reorientation of the methyl group from the SAM-binding site to the solvent, which is linked to the conformation of the side chain of a conserved residue Tyr70.

## INTRODUCTION

Arsenic is the most ubiquitous environmental toxic substance that enters our food and water supply from both geochemical and anthropogenic sources.[1] It poses a serious threat to human health and, consequently, ranks first on the 2017 Environmental Protection Agency's comprehensive environmental response, compensation, and liability act list of hazardous substances (https://www.atsdr.cdc.gov/spl/). This group 1 carcinogen is associated with a number human diseases including lung, bladder, and skin cancers, as well as neuropathy, cardiovascular disease, and diabetes.[2,3] It causes developmental delay in infants and children if the mother is chronically exposed to arsenic during pregnancy or if infants are fed rice baby food containing arsenic (https://www.fda.gov/Food/FoodborneIllnessContaminants/Metals/ucm367263.htm).[4]

Arsenic is acted on biologically, creating an arsenic biogeocycle.[5] Members of every kingdom, from bacteria to humans, biomethylate arsenite, producing the trivalent species methylarsenite (MAs(III)), dimethylarsenite (DMAs(III)) and, to a limited degree, volatile trimethylarsine (TMAs(III)).[1,6] The reaction is catalyzed by the enzyme As(III) SAM methyltransferase (EC 2.1.1.137) (termed ArsM in microbes and AS3MT in animals). In microbes, arsenic methylation is a detoxification process, but in humans, the production of MAs(III) and DMAs(III) has been proposed to increase arsenic toxicity and potentially carcinogenicity.[7,8]

CmArsM from the acidothermoacidophilic eukaryotic red alga *Cyanidioschyzon merolae* sp. 5508 from Yellowstone National Park is a 400-residue thermostable enzyme (44 980 Da, accession number ACN39191) that methylates As(III) to a

Received: February 1, 2018
Accepted: March 2, 2018
Published: March 14, 2018




DOI: 10.1021/acsomega.8b00197
ACS Omega 2018, 3, 3104−3112

final product of volatile TMAs(III), conferring arsenic resistance.[9] Nearly all ArsM orthologs have four conserved cysteine residues, which are Cys44, Cys72, Cys174, and Cys224 in CmArsM (Supporting Information Figure S1).[10,11] Substitution of any of the four eliminates the first methylation step (As(III) to MAs(III)), but either the C44A or C72A derivative is still able to carry out the second step, methylation of MAs(III). Cys44 and Cys72 form a disulfide bond that we hypothesize reduces a transient enzyme-bound pentavalent intermediate, whereas Cys174 and Cys224 form the binding site for trivalent arsenicals. We previously solved the structure of CmArsM to 1.6 Å without ligands and with As(III) or SAM. From a combination of structural and biochemical results, we proposed a catalytic cycle involving a disulfide bond cascade.[12,13]

Here, we determined the rates of the first two steps of methylation, As(III) to MAs(III) and MAs(III) to DMAs (the presumed product, DMAs(III), is rapidly oxidized to DMAs(V) in air, so it will be referred to simply as DMAs in this study). When As(III) was used as the substrate, the first methylation step, As(III) → MAs(III), was rapid, whereas the second methylation step, MAs(III) → DMAs, was considerably slower. In contrast, when methylation was assayed using MAs(III) as the substrate, the rate was somewhat faster than the first methylation step. Thus, the rate of the second methylation step, MAs(III) → DMAs, depends on whether the initial substrate is As(III) or MAs(III). Immediately following the methylation of As(III) to MAs(III), the orientation of the methyl group is inferred to be facing the *S*-adenosylhomocysteine (SAH) product in the SAM-binding site. In order to carry out the next methylation reaction, the methyl group must leave the SAM site to allow a new molecule of SAM to bind. We propose that, when MAs(III) is the product of As(III) methylation, the orientation of the methyl group is adjacent to the SAM-binding site and prevents the SAH product from leaving. This hinders the entrance of another SAM molecule, creating a kinetic block between the first and second methylation steps. To examine the structural basis for this slow step, we obtained several new crystal structures, including MAs(III)-bound CmArsM. In this structure, the orientation of the methyl group is facing toward the solvent, the predicted conformation when MAs(III) is the substrate. In this conformation, an aqueous channel to the active site is occluded, preventing exchange of the product SAH for another SAM substrate. In addition, the aromatic side chain of Tyr70, a residue conserved in most bacterial and animal ArsM orthologs, appears to block the aqueous channel when the arsenic binding site is filled but not when SAM is bound. We propose that slow reorientation of the methyl group from the SAM-binding site to the solvent is rate-limiting in methylation of inorganic arsenic, with the position of the side chain of Tyr70 gating the ligand access.

## RESULTS

**Rate-Limiting Step between the First and Second Methylation Steps.** Methylation was assayed with either As(III) or MAs(III) as the substrate (Figure 1). CmArsM is a heat-stable enzyme; hence, the initial methylation reactions were assayed by HPLC ICP-MS at 60 °C.[14] When As(III) was the substrate, MAs was formed slightly faster than DMAs (Figure 1A, inset), but after 10 min, the amount of MAs decreased, and DMAs continued to increase (Figure 1A) (because the reactions were terminated by the oxidation with $H_2O_2$ to liberate bound products, the oxidation state of the

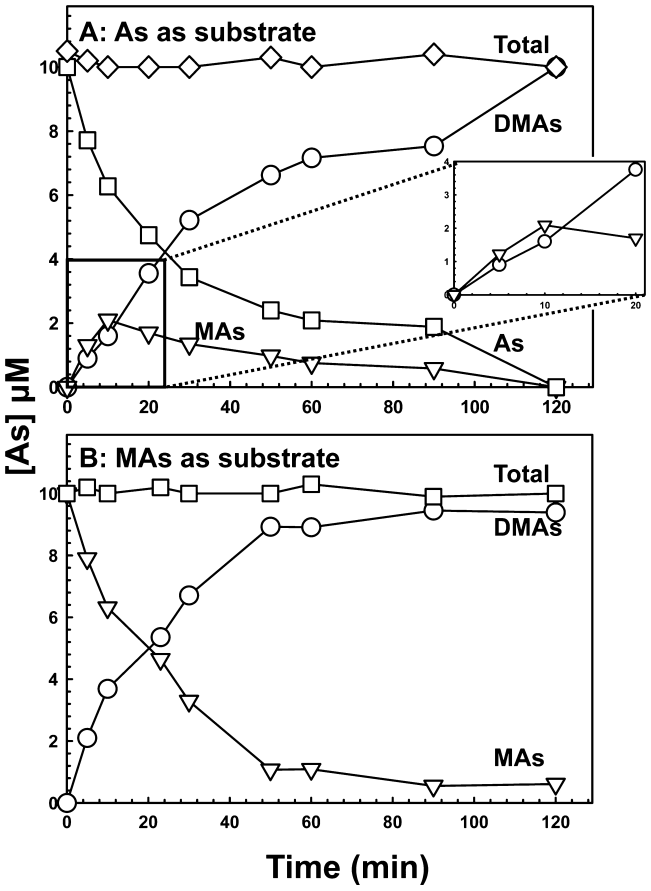


**Figure 1.** Analysis of the first and second steps of CmArsM methylation. Methylation was assayed in a final volume of 1 mL containing 1 mM SAM, 5 mM GSH, 2 μM purified CmArsM, and 10 μM of either As(III) (A) or MAs(III) (B) at 60 °C, as described under Materials and Methods. Samples were withdrawn at the indicated times, and the reaction were terminated by the addition of 10% (v/v) $H_2O_2$, final concentration. Arsenicals were speciated by HPLC-ICP-MS. Inset: As(III) methylation at shorter times.

arsenicals cannot be deduced). When MAs(III) was the substrate, methylation to DMAs was also rapid (Figure 1B). As a thermostable enzyme, CmArsM is much more active at higher temperatures, which makes it difficult to observe the early events. To slow the reaction, the temperature was decreased to 37 °C, and methylation from As(III) to MAs and then to DMAs was assayed. At 37 °C, the conversion of As(III) to MAs was clearly faster than the methylation of As(III) to DMAs (Figure 2). This indicates that the second methylation step (MAs → DMAs) is considerably slower than the first methylation step (As → MAs) when As(III) is the initial substrate. To directly compare the rates of methylation with either As(III) or MAs(III) as the substrate, a FRET assay was used to measure SAH production at 37 °C (Figure 3).[15] In this assay, the rate of conversion of MAs → DMAs with MAs(III) as the substrate was greater or equal to the rate of conversion of As → MAs with As(III) as the substrate. Thus, when As(III) was the substrate, the rate of MAs → DMAs was slower than As → MAs, but with MAs(III) as the substrate, the rate of MAs → DMAs was as fast or faster than As → MAs. These results show that the overall rate of As(III) to DMAs is slower than the individual rates of the first and second methylation reactions, which are intrinsically similar. This demonstrates that there must be a rate-limiting reaction or conformational change



DOI: 10.1021/acsomega.8b00197
ACS Omega 2018, 3, 3104−3112

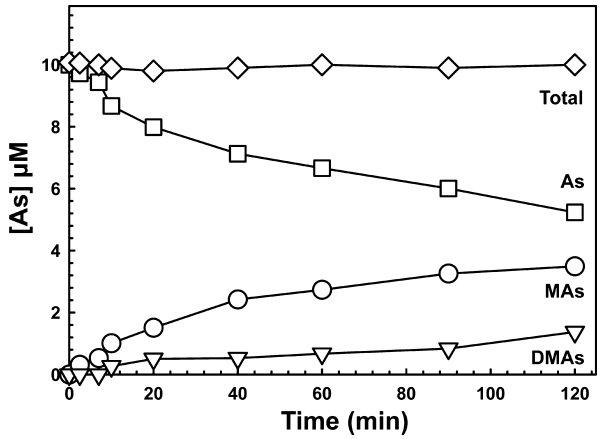


**Figure 2.** As(III) methylation at 37 °C. Methylation was assayed as described in the legend to Figure 1 except that the temperature was 37 °C.

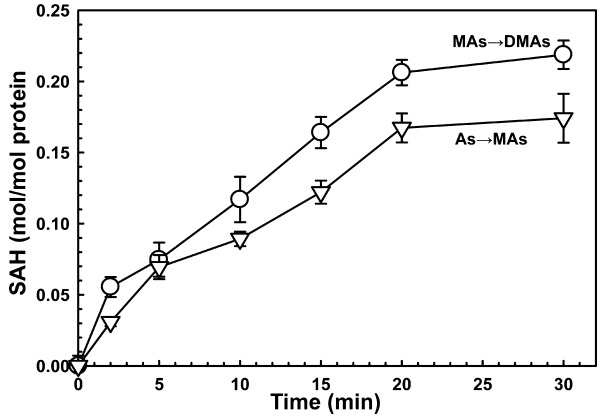


**Figure 3.** Methylation activity with either As(III) or MAs(III). Methylation activity was assayed at 37 °C by conversion of SAM to SAH using a EPIgeneous methyltransferase assay kit (Cisbio Bioassays, Bedford, MA), as described under Materials and Methods. The assay was carried out for the indicated times in 384-well microtiter plates in a buffer consisting of 50 mM $NaH_2PO_4$, pH 8.0, containing 0.3 M NaCl, 2 mM GSH, 1 μM purified CmArsM and 10 μM of either As(III) or MAs(III). SAH production was estimated from the HTRF.

between the addition of the first and second methyl groups. We propose that this slow step involves reorientation of the methyl group of MAs(III) from SAH-facing to solvent-facing.

**New CmArsM Crystal Structures Provide Insights into the Rate-Limiting Step.** To gain insights into the nature of the rate-limiting step, we solved the structure of MAs(III)-bound wild-type CmArsM at 2.27 Å resolution (PDB ID 5JWN). The structural model of the wild-type enzyme with bound MAs(III) contains 328 residues from residue Val50 to Ser371 (Figure 4). An expanded view of the structure shows that MAs(III) is bound to conserved cysteine residues Cys174 and Cys224. The distance between the As atom of MAs(III) and the S atoms of Cys174 and Cys224 is 2.3 and 2.5 Å, respectively. Significantly, the methyl group of MAs(III) is located in an aqueous channel that leads to the solvent, the predicted conformation when MAs(III) is the substrate for a second round of methylation. Biochemical analysis indicates that the binding of SAM during the catalytic cycle produces a conformation of CmArsM that is different from the apo- or arsenical-bound forms.[16] The previously reported SAM-bound

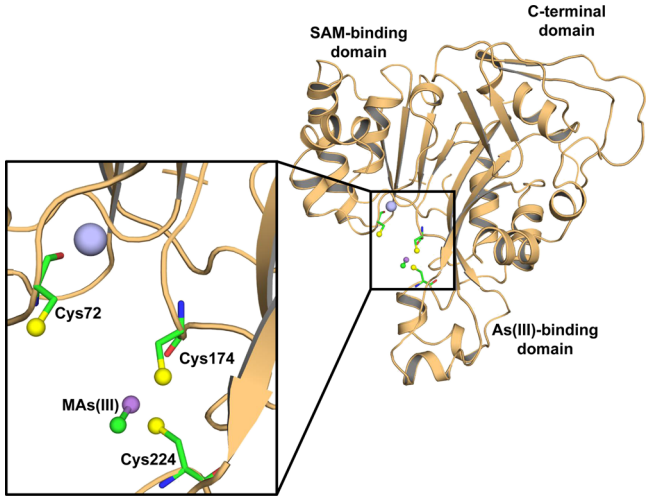


**Figure 4.** Structure of CmArsM with bound MAs(III). Cartoon diagram (colored in light orange) representation of MAs(III)-bound CmArsM (PDB ID 5JWN). The overall structure consists of an N-terminal domain, As(III) binding domain, and a C-terminal domain. Inset: the expanded view of the active site shows the conserved cysteine residues represented by ball-and-stick and colored green (carbon), blue (nitrogen), red (oxygen), or yellow (sulfur). The purple sphere is the arsenic atom, and the light blue sphere is a $Ca^{2+}$ ion found in the SAM-binding site. MAs(III) is bound between conserved residues Cys174 and Cys224.

structure of CmArsM (PDB ID 4FR0) has a loop consisting of residues 51 to 80 that moves 6.3 Å in the direction of the As(III) binding site relative to the MAs(III)-bound structure (Figure 5A).[16] In the SAM-bound CmArsM structure, the distance between the sulfur atoms of Cys74 and Cys170 is 2.1 Å, which suggests the formation of a disulfide bond between those two residues at some step during the catalytic cycle. Superposition of MAs(III)-bound CmArsM and SAM-bound CmArsM gives a root-mean-square distance (rmsd) of 1.25 Å. This high value is consistent with the substantial conformational change caused by the movement of the N-terminal loop toward the As(III)-binding site during catalysis. The distance of the *S*-methyl group of SAM to the As atom of MAs(III) is 4.9 Å (Figure 6A). This orientation indicates that the *S*-methyl group is poised for transferring from SAM to the As atom of MAs(III), the conformation that would be expected during the second round of methylation.

In addition, we solved the structure of a PhAs(III)-bound C72A derivative with an alanine substitution for conserved cysteine residue Cys72 at 1.97 Å resolution (PDB ID 5EG5) (Supporting Information Figure S2). CmArsM is able to methylate aromatic arsenicals such as PhAs(III). Methylation of PhAs(III) is the equivalent of the second methylation step (MAs → DMAs). The structure of PhAs(III)-bound wild-type CmArsM (PDB ID 4KW7) has been previously reported. The benzene ring cannot fit into the space between SAM and the arsenic atom and, as expected, is oriented toward the solvent. The structure of MAs(III)-bound CmArsM is superimposable with PhAs(III)-bound CmArsM with an rmsd of 0.23 Å (Supporting Information Figure S6A). The methyl group of MAs(III) and the benzene ring of PhAs(III) are both oriented toward the solvent, the expected substrate-bound form. In the structure with the trivalent form of the aromatic arsenical poultry growth promoter roxarsone (4-hydroxy-3-nitrobenzenearsenite), the hydroxynitrobenzene ring is similarly oriented.


DOI: 10.1021/acsomega.8b00197
*ACS Omega* 2018, 3, 3104−3112

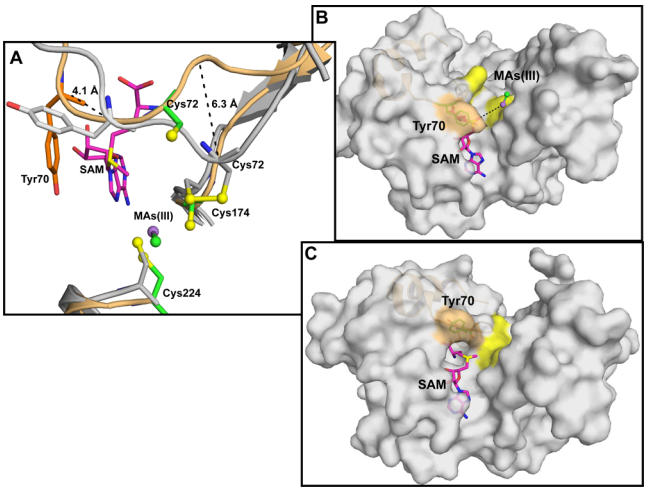


**Figure 5.** Tyr70 gates substrate access to the active site. (A) Superposition of wild-type CmArsM structures with bound MAs(III) (light orange) and bound SAM (light gray) indicates that the main chain ($C^{\alpha}$–$C^{\alpha}$) of Tyr70 differs by 4.1 Å in the two structures. In the SAM-bound structure, Tyr70 is closer to the As(III) binding site than in the MAs(III)-bound structure, suggesting that the hydroxyphenyl side chain of Tyr70 sterically hinders binding of arsenicals when SAM is bound. (B) The surface representation of the MAs(III)-bound structure (light gray) shows that the Tyr70 is in the solvent channel oriented toward the As-binding site and a SAM molecule modeled into the SAM-binding site in ball-and-stick. (C) Surface representation of SAM-bound wild-type CmArsM in the same orientation. In this structure, the side chain of Tyr70 is oriented away from the SAM-binding site, allowing SAM and SAH access to the active site.

Thus, in the structure of CmArsM with three different bound organoarsenicals, the molecule is in the substrate-bound form, and the methylation reaction is the equivalent of the second round of methylation.

The MAs(III)-bound structure includes an N-terminal domain (the SAM-binding domain), a middle As(III)-binding domain, and a C-terminal domain of unknown function. In the PhAs(III)-bound structure of wild-type CmArsM, a disulfide bond is observed between Cys44 and Cys72, which has been proposed to be an obligatory intermediate in the first methylation step. In that structure, the N-terminal domain contains two small $3_{10}$ helices and is followed by a long mobile loop, which moves from the SAM-binding site toward the As(III) binding site during the catalytic cycle. However, the loop containing the conserved residue Cys44 is not resolved in the CmArsM MAs(III)-bound structure, perhaps because it is disordered when the disulfide bond is not present. The electron densities of the bound MAs(III) and conserved cysteine residues Cys174 and Cys224 are shown in Supporting Information Figure S4A. MAs(III) occupancy was partial during several rounds of the structural refinement, with a high temperature factor for MAs(III) (71.61 $Å^2$). The CmArsM-bound MAs(III) structure adopts a pyramidal geometry in which the As atom of MAs(III) is coordinated with the S atoms of Cys174 and Cys224 (Figure 7A). The two S atoms and the C atom of the methyl group are each at an average distance of 3.7 Å from each other. Potential hydrogen bonds and hydrophobic interactions of the protein with the MAs(III) ligand were identified using LigPlot+ analysis (Supporting Information Figure S5A).[17] In addition to the sulfur atoms of Cys174 and Cys224, only Glu223 interacts with the bound ligand.

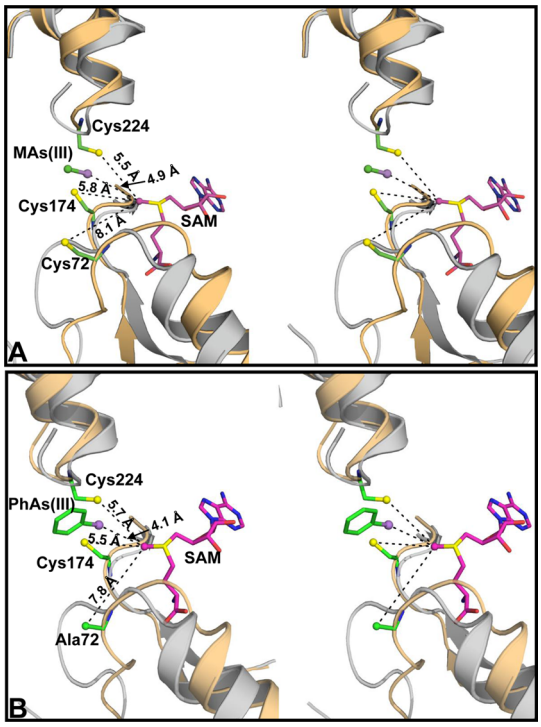


**Figure 6.** Modeling the complex of CmArsM with MAs(III) and SAM. (A) Stereo view of the superimposition of the MAs(III)-bound (light orange) and SAM-bound (light gray) structures, with an rmsd of 1.25 Å. The ternary complex of CmArsM with bound MAs(III) and SAM was modeled by superposition of their individual structures. The distances from the *S*-methyl group of SAM to the sulfur atom of conserved cysteine residues and to the arsenic atom of MAs(III) are indicated. (B) The PhAs(III)-bound C72A structure was superimposed with the SAM-bound wild-type CmArsM structure, with an rmsd of 1.25 Å. The distances of the *S*-methyl group of SAM to the sulfur atom of conserved residues Cys174 and Cys224 and to the arsenic atom of PhAs(III) are indicated. The atoms representation and the coloring are the same as that described in Figure 4.

To further examine the structural basis for the second methylation step, the structure of the PhAs(III)-bound C72A derivative was compared with the MAs(III)-, PhAs(III)-, and SAM-bound structures of wild-type CmArsM. In the C72A structure, PhAs(III) is bound between conserved cysteines residues Cys174 and Cys224 (Supporting Information Figure S3A). The residues are well-defined in the $2F_o$–$F_c$ electron density map contoured at 1.0 $\sigma$. The electron densities of PhAs(III) bound to Cys174 and Cys224 are shown in Supporting Information Figure S4B. The MAs(III)- and C72A PhAs(III)-bound structures can be superposed with an rmsd of 0.24 Å over 322 aligned C$\alpha$ residues (Supporting Information Figure S6A). In both the MAs(III)-bound wild-type CmArsM (Figure 5A) and the PhAs(III)-bound C72A (Supporting Information Figure S3A) structures, the bound organoarsenicals are sandwiched between Tyr70, Glu223, and Gly222. The hydrogen bonds and non-bonded interactions of PhAs(III) with the nearby residues may serve to stabilize the PhAs(III)-bound form (Table 1). Similarly, the PhAs(III)-bound structures of the wild-type CmArsM and C72A proteins are basically superimposable (rmsd of 0.19 Å) (Supporting Information Figure S6B), with similar pyramidal geometries of the PhAs(III) (Figure 7B). The presence of the Cys44–Cys72 disulfide bond in the wild type and its absence in C72A apparently makes no difference in the binding of PhAs(III).



DOI: 10.1021/acsomega.8b00197
*ACS Omega* 2018, 3, 3104–3112

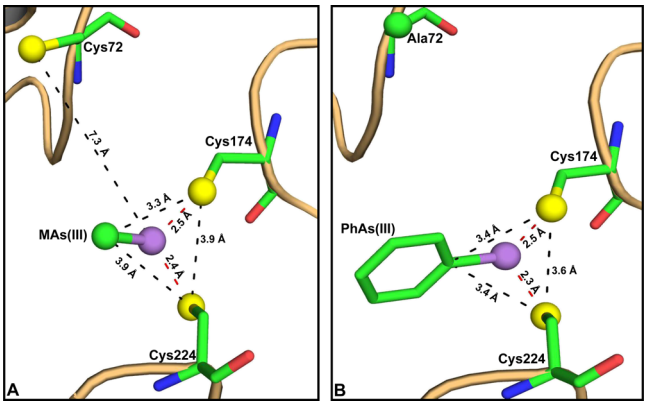


**Figure 7.** Detailed analysis of the As-binding site. (A) MAs(III) is located between conserved residues Cys174 and Cys224 in the MAs(III)-bound structure. In the pyramidal binding site, the distances between the As atom of MAs(III) and the sulfur thiolates of Cys174 and Cys224 are 2.5 and 2.4 Å, respectively. The thiolate of Cys72 is 7.3 Å away from the arsenic atom of MAs(III). The carbon atom of MAs(III) serves as a third arsenic ligand. Each of the liganding atoms are at an average distance of 3.7 Å from each other. (B) PhAs(III) in the C72A structure is located between Cys174 and Cys224. The distances between As atom of PhAs(III) and the sulfur thiolates of Cys174 and Cys224 are 2.5 and 2.3 Å, respectively. In this pyramidal binding site, the central arsenic atom is coordinated with Cys174 and Cys224 at an average distance of 2.4 Å and the C1 carbon atom of PhAs(III) at an average distance of 3.4 Å. Both the methyl group of MAs(III) and the hydroxyphenyl ring of PhAs(III) are oriented toward the solvent channel. The atoms are represented by ball and stick and colored as in Figure 4.

**Table 1. Ligands MAs(III) and PhAs(III) Interaction with Amino Acid Residues Near the Binding Site**

| ligand/atom | amino acid atom | distance (Å) |
|---|---|---|
| | **MAs(III)-Bound CmArsM** | |
| (As) | (O)−C174 | 3.9[b] |
| (As) | (Cβ)−C174 | 3.5[b] |
| (C1) | (S)−C174 | 3.3[a] |
| (C1) | (O)−E223 | 3.6[b] |
| (As) | (Cβ)−C224 | 3.2[a] |
| | **PhAs(III)-Bound C72A** | |
| (C2) | (OH)−Y70 | 3.8[b] |
| (As) | (Cβ)−C174 | 3.2[a] |
| (As) | (O)−C174 | 3.4[a] |
| (C1) | (S)−C174 | 3.4[a] |
| (C6) | (S)−C174 | 3.4[a] |
| (C3) | (O)−G222 | 3.8[b] |
| (C2) | (O)−G222 | 3.6[b] |
| (C3) | (Cα)−E223 | 3.8[b] |
| (As) | (Cβ)−C224 | 3.2[a] |
| (C1) | (Cβ)−C224 | 3.6[b] |
| (C1) | (S)−C224 | 3.4[a] |
| (C2) | (S)−C224 | 3.8[b] |

[a]Moderate hydrogen bonds. [b]Non-bonded interactions between atoms of MAs(III) or PhAs(III) with amino acid atoms.

This is not unexpected because neither Cys72 nor a Cys44−Cys72 disulfide bond is required for the methylation of either MAs(III) or PhAs(III).

The PhAs(III)-bound C72A structure superimposes less well with the wild-type SAM-bound structure (rmsd of 1.25 Å), again because of a difference in the position of the N-terminal loop. The sulfur atoms of Cys174 and Cys224 in the C72A PhAs(III)-bound structure are 7.8, 5.5, and 5.7 Å, respectively, from the *S*-methyl group of SAM in the superimposed structures (Figure 6B). The distance of the *S*-methyl group of SAM to the As atom of PhAs(III) is 4.1 Å, indicating that it is poised for transfer (Figure 6B). The *S*-methyl group of SAM is 7.8 Å distant from the Cβ atom of PhAs(III)-bound C72A. In these structures, the SAM entry is predicted to be restricted in part because the R group of either MAs(III) or PhAs(III) interacts with residues Tyr70, Gly222, and Glu223 (Supporting Information Figure S5) neighboring the As(III) binding site.

**Tyr70 Gates Ligand Binding.** We propose that the orientation of Tyr70 also provides a gating mechanism for substrate access to the active site. In both MAs(III)-bound CmArsM (Figure 5A,B) and PhAs(III)-bound C72A (Supporting Information Figure S3A,B), the hydroxyphenyl ring of Tyr70 is oriented toward the SAM site, but the arsenic binding site is open. In the SAM-bound structure, the Tyr70 side chain is flipped away from the SAM-binding site (Figure 5A,C). In this conformation, the SAM site is open but the arsenic binding site is occluded. This is reflected in a 4.1 Å movement of the Cα of Tyr70 in the SAM-bound structure compared with the MAs(III)-bound wild type enzyme (Figure 5A). In the PhAs(III)-bound C72A structure, this difference is 3.5 Å (Supporting Information Figure 3A). In the SAM-bound structure, the loop that includes Try70 toward the As(III) binding site by 6.3 Å is relative to either the MAs(III)- or PhAs(III)-bound structure. With wild-type CmArsM, this movement brings Cys72 and Cys174 close enough to each other to be able to form the disulfide bond observed in the SAM-bound structure.[16] These results indicate that the Tyr70 hydroxyphenyl ring occludes the aqueous channel to bulk solvent when either MAs(III) or PhAs(III) is bound, preventing the SAM molecule from leaving the active site. In the SAM-bound conformation, the Tyr70 ring is oriented away from the aqueous channel, allowing the exchange of the SAH product for another SAM substrate but forming a Cys72−Cys174 disulfide that prevents binding of arsenicals. We conclude that Tyr70 gates the substrate access to the active site.

## DISCUSSION

Arsenic methylation is a widespread biotransformation process that is catalyzed by the enzyme As(III) *S*-adenosylmethionine methyltransferase. The enzyme methylates trivalent As(III) up to three times, producing mono-, di-, and trimethylated species. In microbes, ArsM clearly catalyzes the detoxification of this toxic metalloid. In humans, arsenic methylation by the orthologous AS3MT has been proposed to transform inorganic arsenic into the more toxic and potentially more carcinogenic[18] species MAs(III) and DMAs(III). When MAs(III) and DMAs(III) are excreted in urine, oxidization by air converts them to the pentavalent species MAs(V) and DMAs(V).[19,20] A high ratio of urinary MAs/DMAs has been associated with various arsenic-related diseases,[21−24] while the reverse appears to be protective.[25] We previously showed that MAs(III), the product of this first methylation step (As(III) → MAs(III)), dissociates very slowly from both human AS3MT[12] and CmArsM.[14] This increases the retention time of MAs(III) in the cytosol of human cells, which may be a critical factor in arsenic toxicity and carcinogenicity. At longer times the second methylation step (MAs(III) → DMAs(III)) predominates, and the major product is the dimethylated species, which rapidly leaves the cells. Thus, the faster the MAs(III) is converted to


DOI: 10.1021/acsomega.8b00197
ACS Omega 2018, 3, 3104−3112

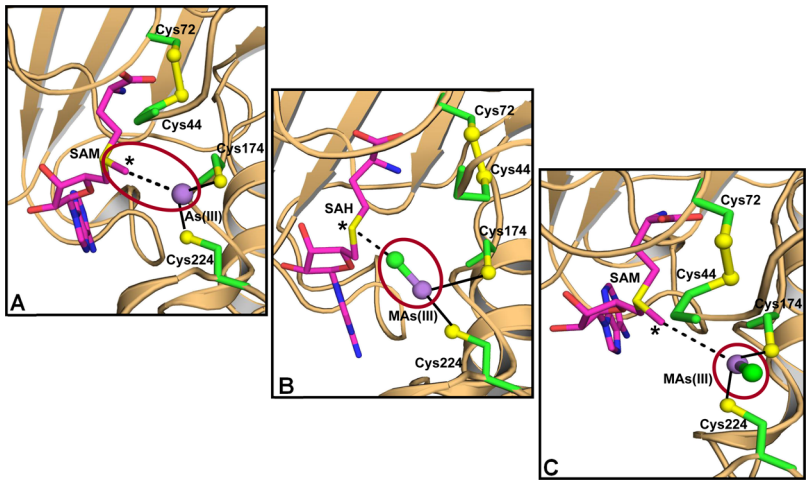


**Figure 8.** Reorientation of the As-methyl group is rate-limiting for catalysis. (A) As(III) is positioned between its binding site composed of Cys174 and Cys224 and the SAM *S*-methyl group. (B) The methyl group is transferred from SAM to As(III), forming a MAs(III)-bound intermediate in which the As-methyl group is oriented toward SAH. (C) Slow reorientation of the As-methyl group toward bulk solvent opens the SAM-binding site, allowing exchange of SAH for SAM. In this conformation, MAs(III) becomes the substrate for the second round of methylation.

DMAs(III), the faster the arsenic can be cleared from the body and the less time it resides inside of cells. It is therefore crucial to understand what governs the ratio of MAs to DMAs, which we predict is related to the catalytic mechanism of AS3MT.

Here, we examined the first two methylation steps in more detail with the AS3MT ortholog CmArsM. With As(III) as the substrate, MAs(III) is formed rapidly, and DMAs(III) more slowly, especially at 37 °C, where the reaction rate is slower. With MAs(III) as the substrate, MAs(III) → DMAs(III) is as rapid as As(III) → MAs(III) when As(III) is the substrate. These results demonstrate that the two steps have intrinsically similar rates, indicating that the slower rate of the second methylation step when As(III) is the substrate is due to a kinetic block that prevents MAs(III) from dissociating from the enzyme. Retaining a substrate in the active site might be expected to accelerate the catalysis because it would eliminate a diffusion-limited step, but that is not the case in this situation. Thus, the MAs(III) product of the first step is not equivalent to the MAs(III) substrate of the second step, even though there is a single active site. We propose that the position of the methyl group in MAs(III) differs in two stages (Figure 8). When As(III) and SAM are both bound, the *S*-methyl group of SAM must face the arsenic atom (Figure 8A). When MAs(III) is the product of As(III) methylation, the methyl group is expected to be located between the sulfur of SAH and the arsenic atom (Figure 8B). For the second methylation to occur, the SAH product must exchange with another molecule of SAM. However, the As-methyl group of the MAs(III) product could sterically clash with the *S*-methyl group of SAM unless it is reoriented away from the SAM-binding site (Figure 8C). Once it attains its new orientation, MAs(III) would become the substrate for the second methylation step. We propose that rate of reorientation of the methyl group is a rate-limiting step between the first and second methylation reactions.

If the rate-limiting step in arsenic methylation in human AS3MT could be overcome, it might be possible to increase the rate of clearance of arsenic from the body, which might diminish the risk of arsenic-related diseases. There are two possibilities to accomplish this goal. One is to utilize allosteric modulators that increase the reaction rate. We identified a potential allosteric site in hAS3MT and are developing small molecule effectors.[15,26] Using this strategy it may be possible to identify activators of hAS3MT in the future. A second strategy is to change residues such as Tyr70 in the active site that are responsible for sterically blocking reorientation of the methyl group. A detailed structure−function analysis of this region of the enzyme is in progress.

## MATERIALS AND METHODS

**Reagents.** All chemicals were obtained from Sigma-Aldrich (St Louis, Missouri, USA) unless otherwise mentioned.

**Purification of CmArsM Enzymes.** CmArsM lacking 31 residues from the N-terminus and 28 residues from the C-terminus with a C-terminal histidine tag (termed simply wild-type CmArsM) was expressed and purified as described previously.[11] The C72A derivative was constructed by site-directed mutagenesis using a QuikChange mutagenesis kit (Stratagene, La Jolla, California, USA). The forward and reverse oligonucleotide primers used for cysteine to alanine mutagenesis (changes underlined) were 5′-GTCCTGGAAAAGTTCTACGGTGCCGGGTCTACGC-3′ and 5′-GCGTAGACCCGGCACCGTAGAACTTTTCCAG-GAC-3′. The mutation was confirmed by sequencing the entire gene. When expressed in *Escherichia coli*, C72A was produced in a soluble form in amounts comparable to the parental CmArsM. Purified enzymes were stored at −80 °C until use. Protein concentrations were estimated from the absorbance at 280 nm. Before crystallization, purified proteins were exchanged into a buffer containing 50 mM MOPS, pH 7.0, containing 0.5 M NaCl and 5 mM dithiothreitol (DTT).

**Cocrystallization of CmArsM and Derivatives with Organoarsenicals.** Crystallization was performed by the hanging drop vapor diffusion method with a variety of crystal screen conditions from Hampton Research (Aliso Viejo, California, USA), Emerald Biosciences Inc. (Bainbridge Island, Washington, USA), and Jena Biosciences GmbH (Jena, Germany).[27] For cocrystallization with MAs(III), 20 μL of wild-type CmArsM at 18 mg/mL was mixed with 20 μL of 2 mM MAs(III) and incubated on ice for 20 min before crystallization. Crystals were obtained by mixing 2.0 μL of protein solutions containing MAs(III) with equal volumes of reservoir solution consisting of 18% PEG 3350, 0.2 M calcium


DOI: 10.1021/acsomega.8b00197
*ACS Omega* 2018, 3, 3104−3112

acetate, and 0.1 M Tris−HCl at pH 7.0. Cocrystallization of C72A with 1 mM phenylarsenite (PhAs(III)) was performed as described previously.[16]

**X-ray Data Collection and Structure Refinement.** Crystals were transferred to a cryoprotectant solution (25% PEG 3350, 0.2 M calcium acetate, 0.1 M Tris−HCl, pH 7.0, and 10% glycerol) and flash-frozen in liquid nitrogen for data collection. Data sets of wild-type MAs(III)-bound CmArsM and PhAs(III)-bound C72A were collected at the southeast regional collaborative access team (SER-CAT) facility at advanced photon source (APS), Argonne National Laboratory. Data were obtained from 360 image frames with 1° rotation angle about $\varphi$ using a MAR-300 CCD detector under standard cryogenic conditions (100 K) at a synchrotron beam line 22-ID with a crystal to detector distance of 200 mm. Data sets were indexed, integrated, and scaled with the HKL2000 suite.[28] Crystals of CmArsM cocrystallized with MAs(III) diffracted at 2.27 Å with the space group of C2, one molecule in the asymmetric unit, and cell parameters of $a$ = 85.56 Å; $b$ = 47.27 Å; $c$ = 100.54 Å; and $\beta$ = 113.9°. Crystals of PhAs(III)-bound C72A diffracted at a resolution of 1.97 Å. The crystals belonged to the monoclinic space group C2 with unit cell parameters of $a$ = 85.26 Å, $b$ = 47.37 Å, $c$ = 100.30 Å, and $\beta$ = 113.6°.

The structures were determined by molecular replacement with Phaser in the CCP4 suite.[29] The unliganded crystal structure of CmArsM (PDB ID 4FS8) was used as a template for molecular replacement. The model and electron density map were visualized using COOT software,[30] and the structure was refined using REFMAC5.[31] The final $R$ and $R_{free}$ converged to 18.9 and 25.7% for MAs(III)-bound CmArsM and 19.5 and 25.0% for PhAs(III)-bound C72A. A Ramachandran plot for MAs(III)-bound CmArsM calculated using PROCHECK[32] indicated that 97.0% of the residues are in the most favored region, 2.4% of the residues in the additionally allowed regions, and 0.6% of the residues in the generously allowed region. The final data collection, refinement statistics, and protein data bank accession codes are given in Table 2. Molecular models were drawn with PYMOL.[33] Ligplot+ was used to illustrate the hydrogen bonds and non-bonded interactions of MAs(III)-bound CmArsM and PhAs(III)-bound C72A.[17]

**Assay of CmArsM Activity.** Methylation activity of purified CmArsM was assayed in 50 mM $NaH_2PO_4$ (pH 8.0) containing 0.3 M NaCl, 5 mM GSH, and 1 mM SAM, as described previously at 60 or 37 °C, as indicated.[14] Unless otherwise noted, the reactions were terminated by adding 10% (v/v) $H_2O_2$, final concentration, to oxidize all arsenic species. Denatured protein was removed by centrifugation using a 3 kDa cut-off Amicon ultrafilter. The products of As(III) or MAs(III) methylation were separated by high-performance liquid chromatography (HPLC) using a Hamilton PRP-X100 C18 reverse phase column (Hamilton Co., Reno, NV) and quantified using a PerkinElmer ELAN DRC-e inductively coupled plasma mass spectrometer (ICP-MS), as described previously.[14]

CmArsM activity was also assayed with an EPIgeneous methyltransferase assay kit (Cisbio Bioassays, Bedford, MA) by measuring the conversion of SAM to SAH as described previously.[15] The reaction has two steps: (1) the enzymatic reaction, which converts SAM to SAH, and (2) the detection step that quantifies SAH production. Both steps were carried out sequentially in the same well of a low volume 384-well microtiter plate, with a total volume of 20 $\mu$L (10 $\mu$L for the enzymatic step and 10 $\mu$L for the detection step) in a buffer consisting of 50 mM $NaH_2PO_4$, pH 8.0, containing 0.3 M NaCl, 2 mM GSH, 1 $\mu$M CmArsM, and 10 $\mu$M of either As(III) or MAs(III). After incubating for 1 min, 10 $\mu$M SAM, final concentration, was added to initiate the reaction. The reactions were carried out at 37 °C for the indicated times. The reactions were terminated by addition of the proprietary detection reagent, followed by SAH-d2 and anti-SAH-Lumi4-Tb reagents. Fluorescence was measured at both 665 and 620 nm with excitation at 337 nm in a Synergy H4 Hybrid Multi-Mode Microplate Reader. The homogeneous time-resolved fluorescence (HTRF) was calculated from the ratio of emission at 665 and 620 nm. The concentration of SAH was calculated

**Table 2. Data Collection, Indexing, and Refinement Statistics**[a]

| data collection | MAs(III)-bound CmArsM | PhAs(III)-bound C72A |
|---|---|---|
| diffraction source | APS 22-ID | APS 22-ID |
| wavelength (Å) | 1.0 | 1.0 |
| detector | MARCCD 300 | MARCCD 300 |
| space group | C2 | C2 |
| $a$, $b$, $c$ (Å) | 85.56, 47.27, 100.54 | 85.26, 47.37, 100.26 |
| $\alpha$, $\beta$, $\gamma$ (deg) | 90.0, 113.9, 90.0 | 90.0, 113.6, 90.0 |
| resolution range (Å) | 100−2.27 (2.37−2.27) | 50.0−1.97 (2.04−1.97) |
| unique reflections | 17 063 (1624) | 23 355 (2467) |
| completeness (%) | 99.2 (95.1) | 89.7 (96.9) |
| redundancy | 7.3 (6.4) | 7.2 (7.4) |
| $(I)/\sigma(I)$ | 26.6 (7.3) | 20.1 (8.6) |
| [b]$R_{sym.}$ | 0.057 (0.205) | 0.054 (0.235) |
| [c]$R_{r.i.m.}$ | 0.053 (0.223) | 0.058 (0.253) |
| [d]$R_{p.i.m}$ | 0.019 (0.085) | 0.022 (0.092) |
| Wilson $B$-factor (Å$^2$) | 34.4 | 22.8 |
| | [f]Refinement | |
| [e]$R_{work}$/(%) | 18.9 (26.6) | 19.5 (22.0) |
| [e]$R_{free}$ (%) | 25.7 (38.8) | 25.0 (27.2) |
| no. of atoms | 2619 | 2730 |
| macromolecules | 2536 | 2539 |
| ligands | 3 | 8 |
| water | 80 | 183 |
| RMS (bonds) (Å$^2$) | 0.016 | 0.016 |
| RMS (angles) (deg) | 1.732 | 1.84 |
| [g]Ramachandran favored (%) | 97.0 | 97.0 |
| Ramachandran allowed (%) | 2.38 | 2.07 |
| Ramachandran outliers (%) | 0.62 | 0.93 |
| average $B$-factor (Å$^2$) | 42.20 | 35.30 |
| macromolecules | 42.40 | 35.30 |
| ligands | 45.10 | 44.60 |
| water | 37.60 | 38.50 |
| PDB code | 5JWN | 5EG5 |

[a]Values in parenthesis are for the highest resolution bin. [b]$R_{merge} = \Sigma_{hkl}\Sigma_i|I_{i,hkl} - \overline{I}_{hkl}|/\Sigma_{hkl}\Sigma_i|I_{i,hkl}|$, where $I_i(hkl)$ is the observed intensity and $I(hkl)$ is the average intensity over symmetry equivalent measurements. [c]$R_{r.i.m.} = \Sigma_{hkl}(N/(N-1))^{1/2}\Sigma_i|I_{i,hkl} - \overline{I}_{hkl}|/\Sigma_{hkl}\Sigma_i|I_{i,hkl}|$. [d]$R_{p.i.m.} = \Sigma_{hkl}(1/(N-1))^{1/2}\Sigma_i|I_{i,hkl} - \overline{I}_{hkl}|/\Sigma_{hkl}\Sigma_i|I_{i,hkl}|$. [e]$R_{work} = \Sigma_{hkl}|IF_{obs}I - IF_{cal}I|/\Sigma_{hkl}|IF_{obs}I$, where $R$ free is calculated for a random chosen 5% of reflections which were not used for structure refinement, and $R$ work is calculated for the remaining reflections. [f]Refinement using REFMAC.[23] [g]Ramachandran plot calculated using PROCHECK.[24]



DOI: 10.1021/acsomega.8b00197
ACS Omega 2018, 3, 3104−3112

from a calibration curve of the HTRF with known concentrations of SAH.

## ■ ASSOCIATED CONTENT

### Supporting Information

The Supporting Information is available free of charge on the ACS Publications website at DOI: 10.1021/acsomega.8b00197.

Multiple sequence alignment of As(III) SAM methyltransferases; structure of the CmArsM C72A derivative with bound PhAs(III); superposition of the structures of C72A with bound PhAs(III) and SAM-bound wild-type CmArsM; stereo view of electron density map of (A) MAs(III) and (B) mutant C72A bound-PhAs (III) in CmArsM; residues interacting with MAs(III) or PhAs-(III); and superimposition of MAs(III)- and PhAs(III)-bound structures (PDF)

## ■ AUTHOR INFORMATION


### Corresponding Author

*E-mail: brosen@fiu.edu. Phone: 305-348-0657. Fax: 305-348-0651 (B.P.R.).

### ORCID

Barry P. Rosen: 0000-0002-5230-4271


### Notes

The authors declare no competing financial interest.

## ■ ACKNOWLEDGMENTS

This work was supported by NIH grants GM55425 and ES023779 and a Pilot Project award to C.P. from the Herbert Wertheim College of Medicine. This project utilized the Southeast Regional Collaborative Access Team (SER-CAT) 22-ID beam line of the Advanced Photon Source, Argonne National Laboratory. Use of the Advanced Photon Source was supported by the US Department of Energy, Office of Science and Office of Basic Energy Sciences under contract no. W-31-109-Eng-38. The Berkeley Center for Structural Biology is supported in part by the National Institutes of Health, National Institute of General Medical Sciences, and the Howard Hughes Medical Institute. The Advanced Light Source is supported by the Director, Office of Science, Office of Basic Energy Sciences of the US Department of Energy under Contract no. DE-AC02-05CH11231.

## ■ REFERENCES


(1) Zhu, Y.-G.; Yoshinaga, M.; Zhao, F.-J.; Rosen, B. P. Earth abides arsenic biotransformations. *Annu. Rev. Earth Planet. Sci.* **2014**, *42*, 443−467.

(2) Abernathy, C. O.; Thomas, D. J.; Calderon, R. L. Health effects and risk assessment of arsenic. *J. Nutr.* **2003**, *133*, 1536S−1538S.

(3) Mateen, F. J.; Grau-Perez, M.; Pollak, J. S.; Moon, K. A.; Howard, B. V.; Umans, J. G.; Best, L. G.; Francesconi, K. A.; Goessler, W.; Crainiceanu, C.; Guallar, E.; Devereux, R. B.; Roman, M. J.; Navas-Acien, A. Chronic arsenic exposure and risk of carotid artery disease: The Strong Heart Study. *Environ. Res.* **2017**, *157*, 127−134.

(4) Farzan, S. F.; Karagas, M. R.; Chen, Y. In utero and early life arsenic exposure in relation to long-term health and disease. *Toxicol. Appl. Pharmacol.* **2013**, *272*, 384−390.

(5) Zhu, Y.-G.; Xue, X.-M.; Kappler, A.; Rosen, B. P.; Meharg, A. A. Linking genes to microbial biogeochemical cycling: lessons from arsenic. *Environ. Sci. Technol.* **2017**, *51*, 7326−7339.

(6) Thomas, D. J.; Rosen, B. P. Arsenic methyltransferases. In *Encyclopedia of Metalloproteins*; Kretsinger, R. H., Uversky, V. N., Permyakov, E. A., Eds.; Springer: New York, NY, 2013; pp 138−143.

(7) Styblo, M.; Razo, L. M. D.; Vega, L.; Germolec, D. R.; LeCluyse, E. L.; Hamilton, G. A.; Reed, W.; Wang, C.; Cullen, W. R.; Thomas, D. J. Comparative toxicity of trivalent and pentavalent inorganic and methylated arsenicals in rat and human cells. *Arch. Toxicol.* **2000**, *74*, 289−299.

(8) Petrick, J. S.; Ayala-Fierro, F.; Cullen, W. R.; Carter, D. E.; Aposhian, H. V. Monomethylarsonous acid (MMA(III)) is more toxic than arsenite in Chang human hepatocytes. *Toxicol. Appl. Pharmacol.* **2000**, *163*, 203−207.

(9) Qin, J.; Lehr, C. R.; Yuan, C.; Le, X. C.; McDermott, T. R.; Rosen, B. P. Biotransformation of arsenic by a Yellowstone thermoacidophilic eukaryotic alga. *Proc. Natl. Acad. Sci. U.S.A.* **2009**, *106*, 5213−5217.

(10) Packianathan, C.; Pillai, J. K.; Riaz, A.; Kandavelu, P.; Sankaran, B.; Rosen, B. P. Crystallization and preliminary X-ray crystallographic studies of CrArsM, an As(III) S-adenosylmethionine methyltransferase from Chlamydomonas reinhardtii. *Acta Crystallogr., Sect. F: Struct. Biol. Commun.* **2014**, *70*, 1385−1388.

(11) Marapakala, K.; Ajees, A. A.; Qin, J.; Sankaran, B.; Rosen, B. P. Crystallization and preliminary X-ray crystallographic analysis of the ArsM arsenic(III) S-adenosylmethionine methyltransferase. *Acta Crystallogr., Sect. F: Struct. Biol. Commun.* **2010**, *66*, 1050−1052.

(12) Dheeman, D. S.; Packianathan, C.; Pillai, J. K.; Rosen, B. P. Pathway of human AS3MT arsenic methylation. *Chem. Res. Toxicol.* **2014**, *27*, 1979−1989.

(13) Marapakala, K.; Packianathan, C.; Ajees, A. A.; Dheeman, D. S.; Sankaran, B.; Kandavelu, P.; Rosen, B. P. A disulfide-bond cascade mechanism for As(III) S-adenosylmethionine methyltransferase. *Acta Crystallogr., Sect. D: Biol. Crystallogr.* **2015**, *71*, 505−515.

(14) Marapakala, K.; Qin, J.; Rosen, B. P. Identification of catalytic residues in the As(III) S-adenosylmethionine methyltransferase. *Biochemistry* **2012**, *51*, 944−951.

(15) Dong, H.; Xu, W.; Pillai, J. K.; Packianathan, C.; Rosen, B. P. High-throughput screening-compatible assays of As(III) S-adenosylmethionine methyltransferase activity. *Anal. Biochem.* **2015**, *480*, 67−73.

(16) Ajees, A. A.; Marapakala, K.; Packianathan, C.; Sankaran, B.; Rosen, B. P. Structure of an As(III) S-adenosylmethionine methyltransferase: insights into the mechanism of arsenic biotransformation. *Biochemistry* **2012**, *51*, 5476−5485.

(17) Laskowski, R. A.; Swindells, M. B. LigPlot+: multiple ligand-protein interaction diagrams for drug discovery. *J. Chem. Inf. Model.* **2011**, *51*, 2778−2786.

(18) Sty'blo, M.; Drobná, Z.; Jaspers, I.; Lin, S.; Thomas, D. J. The role of biomethylation in toxicity and carcinogenicity of arsenic: a research update. *Environ. Health Perspect.* **2002**, *110*, 767−771.

(19) Gong, Z.; Lu, X.; Cullen, W. R.; Le, X. C. Unstable trivalent arsenic metabolites, monomethylarsonous acid and dimethylarsinous acid. *J. Anal. At. Spectrom.* **2001**, *16*, 1409−1413.

(20) Le, X. C.; Lu, X.; Ma, M.; Cullen, W. R.; Aposhian, H. V.; Zheng, B. Speciation of key arsenic metabolic intermediates in human urine. *Anal. Chem.* **2000**, *72*, 5172−5177.

(21) Vahter, M. Mechanisms of arsenic biotransformation. *Toxicology* **2002**, *181−182*, 211−217.

(22) Antonelli, R.; Shao, K.; Thomas, D. J.; Sams, R., 2nd; Cowden, J. AS3MT, GSTO, and PNP polymorphisms: impact on arsenic methylation and implications for disease susceptibility. *Environ. Res.* **2014**, *132*, 156−167.

(23) Engström, K. S.; Vahter, M.; Fletcher, T.; Leonardi, G.; Goessler, W.; Gurzau, E.; Koppova, K.; Rudnai, P.; Kumar, R.; Broberg, K. Genetic variation in arsenic (+3 oxidation state) methyltransferase (AS3MT), arsenic metabolism and risk of basal cell carcinoma in a European population. *Environ. Mol. Mutagen.* **2015**, *56*, 60−69.

(24) Huang, Y.-K.; Tseng, C.-H.; Huang, Y.-L.; Yang, M.-H.; Chen, C.-J.; Hsueh, Y.-M. Arsenic methylation capability and hypertension risk in subjects living in arseniasis-hyperendemic areas in southwestern Taiwan. *Toxicol. Appl. Pharmacol.* **2007**, *218*, 135−142.




DOI: 10.1021/acsomega.8b00197
*ACS Omega* 2018, 3, 3104−3112

(25) Engström, K. S.; Broberg, K.; Concha, G.; Nermell, B.; Warholm, M.; Vahter, M. Genetic polymorphisms influencing arsenic metabolism: evidence from Argentina. *Environ. Health Perspect.* **2007**, *115*, 599−605.
(26) Dong, H.; Madegowda, M.; Nefzi, A.; Houghten, R. A.; Giulianotti, M. A.; Rosen, B. P. Identification of small molecule inhibitors of human As(III) S-adenosylmethionine methyltransferase (AS3MT). *Chem. Res. Toxicol.* **2015**, *28*, 2419−2425.
(27) McPherson, A. Current approaches to macromolecular crystallization. *Eur. J. Biochem.* **1990**, *189*, 1−23.
(28) Otwinowski, Z.; Minor, W. Processing of X-ray diffraction data collected in oscillation mode. *Methods Enzymol.* **1997**, *276*, 307−326.
(29) McCoy, A. J. Solving structures of protein complexes by molecular replacement with Phaser. *Acta Crystallogr., Sect. D: Biol. Crystallogr.* **2007**, *63*, 32−41.
(30) Emsley, P.; Cowtan, K. Coot: model-building tools for molecular graphics. *Acta Crystallogr., Sect. D: Biol. Crystallogr.* **2004**, *60*, 2126−2132.
(31) Vagin, A. A.; Steiner, R. A.; Lebedev, A. A.; Potterton, L.; McNicholas, S.; Long, F.; Murshudov, G. N. REFMAC5 dictionary: organization of prior chemical knowledge and guidelines for its use. *Acta Crystallogr., Sect. D: Biol. Crystallogr.* **2004**, *60*, 2184−2195.
(32) Laskowski, R. A.; Rullmann, J. A. C.; MacArthur, M. W.; Kaptein, R.; Thornton, J. M. AQUA and PROCHECK-NMR: programs for checking the quality of protein structures solved by NMR. *J. Biomol. NMR* **1996**, *8*, 477−486.
(33) DeLano, W. L. *The PyMOL User's Manual*; DeLano Scientific: San Carlos, CA, 2001.



DOI: 10.1021/acsomega.8b00197
*ACS Omega* 2018, 3, 3104−3112